Biology and Fertility of Soils (2021) 57:587–601
https://doi.org/10.1007/s00374-021-01551-7

ORIGINAL PAPER

The mineralosphere—interactive zone of microbial colonization and carbon use in grassland soils

Runa S. Boeddinghaus[1,2] · Sven Marhan[1] · Aurelia Gebala[1] · Heike Haslwimmer[1] · Selma Vieira[3] · Johannes Sikorski[3] · Jörg Overmann[3] · Margarida Soares[4,5] · Johannes Rousk[4] · Thilo Rennert[6] · Ellen Kandeler[1]

Received: 30 October 2020 / Revised: 19 February 2021 / Accepted: 4 March 2021 / Published online: 12 March 2021

Abstract

To improve our understanding of early microbial colonization of pristine minerals and their group-specific C utilization, we exposed minerals (illite/goethite/quartz) amended with artificial root exudates (ARE, glucose, and citric acid) in grassland soils for a period of 24 weeks. FTIR spectra indicated that mineral-associated ARE were used within the first 2 weeks of exposure and were replaced by other carbohydrates derived from living or dead cells as well as soil-borne C sources transported into the mineralosphere after heavy rain events. Fungi and Gram-positive bacteria incorporated ARE-derived C more rapidly than Gram-negative bacteria. Gram-negative bacteria presumably profited indirectly from the ARE by cross-feeding on mineral-associated necromass of fungi and Gram-positive bacteria. The Gram-negative bacterial phyla *Verrucomicrobia*, *Planctomycetes*, *Gemmatimonadetes*, *Armatimonadetes*, and *Chloroflexi* showed a positive correlation with Gram-negative PLFA abundances. After 24 weeks of exposure in the grassland soils, abundances of soil microorganisms in the mineralosphere reached only 3.1% of the population density in soil. In conclusion, both bacteria and fungi slowly colonize new surfaces such as pristine minerals, but quickly assimilate artificial root exudates, creating an active microbial community in the mineralosphere.

Keywords Minerals · Soil microorganisms · Exudates · Meadow · Pasture · Carbon turnover

Introduction

The survival and functioning of soil microorganisms in terrestrial ecosystems depend on interactions between biotic and abiotic (chemical and physical) components of the soil (Erktan et al. 2020; Seaton et al. 2020). Whereas the colonization of some microhabitats, such as the rhizosphere, detritusphere, and drilosphere, is well studied under natural environmental conditions (Hünninghaus et al. 2019; Johnson-Maynard and Strawn 2016; Poll et al. 2008), studies of the microbial life associated with minerals are rare. The surface of soil minerals represents a biogeochemical interface, where the organic and inorganic constituents of the soil come together (Totsche et al. 2010). Besides the fundamental work of Stotzky (1986) about microbial associations to soil minerals, Uroz et al. (2015) provided a conceptual framework of the importance of microorganisms colonizing clay-sized minerals (< 2 µm), which are the most reactive inorganic soil constituents. They defined the mineralosphere as the specific interface and habitat encompassing mineral surfaces and the surrounding soil, i.e., the sphere that is physically, chemically, and biologically influenced by minerals. The focus of previous studies on microbe-mineral interactions improved our understanding of mineral weathering (Ahmed and Holmström 2015; Hagenberg et al. 2003), microbial colonization of

✉ Sven Marhan
sven.marhan@uni-hohenheim.de

1 Institute of Soil Science and Land Evaluation, Department of Soil Biology, University of Hohenheim, 70599 Stuttgart, Germany

2 Landwirtschaftliches Technologiezentrum Augustenberg (LTZ), 76227 Karlsruhe, Germany

3 Leibniz Institute DSMZ-German Collection of Microorganisms and Cell Cultures, Inhoffenstraße 7B, 38124 Brunswick, Germany

4 Department of Biology, Microbial Ecology, Lund University, 22362 Lund, Sweden

5 Department of Biology, Aquatic Ecology, Lund University, 22362 Lund, Sweden

6 Institute of Soil Science and Land Evaluation, Department of Soil Chemistry and Pedology, University of Hohenheim, 70599 Stuttgart, Germany

different minerals (Sun et al. 2020), and the decomposition of mineral-associated organic matter (Chenu and Stotzky 2002; Wang et al. 2019). However, studies investigating the mineralosphere in a natural soil are limited (Leinemann et al. 2018; Wang et al. 2017; Whitman et al. 2018).

In natural environments, not only the types of minerals but also the amount and composition of organic substrates play important roles in the abilities of different soil microorganisms to colonize the mineralosphere. While rather poorly degradable C resources enter soils mainly as plant debris such as leaf and root litter, labile C resources originate mainly from rhizodeposition, which is a major source of C for soil microorganisms (Liliensiek et al. 2012). The most labile C components in rhizodeposition are root exudates (Grayston et al. 1997), which consist predominantly of sugars, amino acids, and organic acids (van Hees et al. 2005). They are known to increase soil microbial activity and abundance and to affect microbial community composition (Grayston et al. 1997; Rovira 1969; Strickland et al. 2015; Vieira et al. 2020). Glucose, glycine, and oxalic and citric acids have frequently been used to study the microbial response after addition of artificial root exudates (Eilers et al. 2010; Strickland et al. 2015). Any organic compound entering the mineralosphere may be either directly bound to pristine minerals or first processed by microorganisms with subsequent adsorption to mineral surfaces.

Microorganisms in the mineralosphere have two different and opposing functions in the C cycling of mineral-associated organic substances: microbial assimilation of mineral-associated organic substances and oxidation and depolymerization of SOM promoting the formation of SOM-mineral associations leading to SOM stabilization (Lehmann et al. 2020; Wang et al. 2017). The concept of using artificial soils to create a pristine environment for soil development has been used (Babin et al. 2013, 2014; Ditterich et al. 2016; Hemkemeyer et al. 2014; Kallenbach et al. 2016; Vogel et al. 2014) to study the composition, succession, and C use of soil microorganisms as they colonize pristine organo-mineral surfaces. Babin et al. (2014) detected differences in bacterial and fungal community composition of artificial soils amended with easily available vs. rather complex C resources. Stable-isotope techniques (SIP) have made it possible to track C flow from substrates into different groups of microorganisms in soils (Kramer et al. 2016; Paterson et al. 2008). These studies yielded evidence of group-specific use of labile and complex C sources. The study of Kandeler et al. (2019) is one of the first to explore microbial succession and C use by mineral-associated microorganisms under field conditions. Microorganisms colonizing mineral containers (illite/goethite/quartz) for up to 2.5 years had access to labeled *Dactylis glomerata* and *Lolium perenne* roots as a complex substrate. Fungi colonized pristine mineral surfaces in grassland soils more rapidly than bacteria because hyphae reached and assimilated substrates associated with new surfaces faster than bacteria, which rely primarily on passive transport in soil. Furthermore, mineral-associated microorganisms were more active than those microorganisms in the bulk soil of the grassland sites (Kandeler et al. 2019).

Nevertheless, information on the dynamics of C incorporation into mineral-associated microorganisms that have access to easily available root exudates bound to minerals under field conditions is lacking. Our approach exposed organo-mineral complexes, represented by pristine minerals loaded with ARE, in mineral containers in the topsoil of ten grassland sites of different land-use intensities of the Biodiversity Exploratories at the Schwäbische Alb (south-west Germany). Whereas Vieira et al. (2020) used the same experimental set-up as the present study to describe bacterial community succession during one season, we present high-resolution temporal data on both the succession of organic compounds associated with minerals and of bacterial and fungal C use dynamics over one growth season. Specifically, we hypothesized that (1) the mineral-associated organic matter will be modified by colonizing microorganisms and/or by the input of soil-derived DOC; (2) both bacteria and fungi will use the ARE-derived C in the early phases of mineral colonization, but fungi will reach the minerals and the substrate faster than bacteria due to their hyphal growth pattern; and (3) soil-derived C from the local environment of grassland sites will be substituted for the ARE-derived C in bacteria and fungi in the later phases of exposure, and the extent of this C replacement may depend on the land-use intensity of the grasslands. Further, the substitution process may be specific to individual groups of soil microorganisms (Gram-positive bacteria, Gram-negative bacteria, and fungi).

Material and methods

Study sites

The experimental sites are part of the long-term research platform German Biodiversity Exploratories (Fischer et al. 2010) (www.biodiversity-exploratories.de) and are continuously farmed by their owners under different land-use intensities (LUI). We selected five low and five high LUI grassland sites according to the LUI index developed by Blüthgen et al. (2012). Sites characterized by low LUI were not fertilized, mown only once a year, and grazed by sheep for one to 5 days per year, mainly in early summer or early autumn (Table S1). High LUI sites were highly fertilized and mown three times a year or were intensively grazed by cattle, horses, or both. In addition to LUI, experimental sites were selected for similar climatic conditions, soil type, and soil pH (Kandeler et al. 2019). The soils at all sites were Rendzic Leptosols (IUSS Working Group WRB 2015) with an average pH of 6.4 (pH range 5.7–7.0). The sum of precipitation and average daily temperature during the experiment (May to November 2015) were 328 mm and 8.6 °C, respectively (Fig. S1). Total C and N contents differed between the sites based on their LUI (Boeddinghaus et al. 2019) with C and N content of 74.7 g C kg^{-1} soil and 6.3 g N kg^{-1} soil in low and 71.7 g C kg^{-1} soil and 7.2 g N kg^{-1} soil in high LUI sites. This resulted in a C/N ratio of 11.0 for low LUI as compared to 9.8 for high LUI sites.

Experimental design

The field experiment was installed on 4 × 4 m plots within each of the ten grassland sites. The 16 m^2 area was divided into 64 equal subplots of 25 × 25 cm. On May 28, 2015, we buried 15 containers filled with an ARE-loaded mineral mixture, each in one randomly chosen subplot per plot. A soil block of about 18 × 18 cm and 8 cm depth was excavated with a spade in the center of each subplot, and a mineral container was laterally inserted into the main rooting zone (Fig. S2). The containers were composed of polyvinyl chloride (PVC) with a diameter of 7 cm and a height of 1 cm. Tops and bottoms of the containers were covered with 50 μm mesh gauze (SEFAR NITEX®, Sefar AG Heiden, Switzerland), which excludes roots but enables microbial invasion and thereby colonization. The containers were filled with 30.8 g mineral mixture. This mixture was artificially mixed to resemble the qualitative and quantitative composition of Rendzic Leptosols and consisted of 71.4% illite (Inter-ILI Mérnöki Iroda, Hungary), 9.6% goethite (Bayferrox® 920, Lanxess Deutschland GmbH, Köln, Germany), 17% silt-sized (Millsil W11 H), and 2% sand-sized (Quartz Sand Haltern, H33) quartz (Quarzwerke GmbH Frechen, Germany) (see Kandeler et al. 2019). The quantity of minerals in the containers was adjusted to conform to the average top soil bulk density (0.75 g cm^{-3}) of the ten sites (Boeddinghaus et al. 2019). The pure mineral mixture was characterized, per gram dry mass, by 1.49 μg exchangeable NH_4^+-N, 0.04 μg NO_3^--N, 8 μg P, 437 μg K, 0.34 mg C_{org}, and 0.12 mg N_t and a pH of 5.3. Exchangeable NH_4^+-N, NO_3^--N, and N_t were analyzed as described in Kandeler et al. (2019). Plant-available P and K were extracted according to Bray and Kurtz (1945) and pH was measured in 0.01 M $CaCl_2$ solution. The relative distribution of exchangeable cations was 0.3% (Na), 10.3% (K), 25.2% (Mg), and 65.2% (Ca). Given the parent material of the soils and the pH conditions, we can exclude distinct changes in the distribution of these cations. Particularly, we can exclude the initial presence of exchangeable Al ions or their accumulation during the field exposure. As the point of zero charge of Fe oxides is > 7, we can take little positive charge on the goethite surface as given, balanced by adsorbed anions.

The pure mineral mixture of each container was loaded with 2.95 mg glucose and 1.37 mg citric acid, as these are amongst the main substances excreted by roots (Rovira 1969). The ARE consisted of 68% $^{13}C_6$-labeled glucose (CAS Number 110187-42-3, Sigma-Aldrich Chemie GmbH, Munich, Germany) and 32% $^{13}C_6$ citric acid (CAS Number 287389-42-8, Sigma-Aldrich Chemie GmbH, Munich, Germany), which were diluted 1:4 beforehand with unlabeled ^{12}C glucose and citric acid, respectively. To avoid nutrient limitation, we added ammonium nitrate to ensure a similar C:N ratio in the mineral mixtures to that of the topsoil of the ten grassland sites (C:N ratio mineral mixture = 10, average across ten sites = 10.4) and to be within the average rate of C:N ratios of root exudates of 2.5 to 13 as summarized by Grayston et al. (1997). To ensure attachment of the ARE to the mineral mixture, we dissolved ARE and ammonium nitrate in 0.01 M $CaCl_2$ and pipetted 15 ml of this solution into the 30.8 g mineral mixture, ensuring uniform moistening by avoiding leaching. When fresh ARE mineral mixtures were tested by rinsing with water, a maximum C loss of only 5% was found. The mineral mixtures were not sterilized, as this can change the physical and chemical properties of the mineral mixture and the ARE (Berns et al. 2008; McNamara et al. 2003). The bacterial community of the original mineral mixtures was investigated in detail in a previous study (Vieira et al. 2020), showing that most of the bacterial sequence variants detected in the mineral mixtures after exposure were not present before the burial of the minerals. C_{mic} and PLFA abundances were both detectable in the original mineral mixture, but were much lower than after exposure (Table S1).

Sampling design

Three randomly selected containers were excavated from each grassland site two (June 11, 2015), four (June 25, 2015), nine (July 27, 2015), 17 (September 24, 2015), and 24 (November 11, 2015) weeks after the start of the experiment. In addition to the mineral containers ("minerals"), "adjacent soil" samples were taken, consisting of the pooled soil sampled within 1 cm above and below the containers. As a third sample, "control" soil samples were taken randomly from three subplots in each grassland site without container addition at 7 cm depth. All samples were transported on ice bags in cooling boxes to the laboratory and stored at 4 °C until further preparation. In the laboratory, we controlled potential root ingrowth into the mesh of mineral containers by microscopic inspection. We could not detect any root ingrowth; consequently, only very fine roots might have contributed to the organic matter inside the mineral containers. Three samples from each type (minerals, adjacent soil, control) were combined plot-wise during sieving. Minerals were sieved < 2 mm; soil samples were sieved < 5 mm and roots and stones were removed. After sample preparation, aliquots were stored at -24 °C for further analysis. Gravimetric water contents of soil and mineral samples were determined by drying 5 g of sample at 60 °C for at least 72 h to constant mass.

Field measurements

Precipitation and air temperature 2 m above ground, as well as soil moisture and soil temperature at 10 cm depth, were recorded at the sites using an ADL-MX Datalogger System equipped with DeltaT ML2X Soil Humidity Probe, MNT FExtension 2010 Soil and Ground Surface Temperature Sensor, and a MELA KPC1/5-ME & #IAK1.00.F137.520.CS8 Humidity and Air Temperature Sensor (Biodiversity Exploratories Instrumentation Project (BExIS dataset ID 19007)). As precipitation was only recorded on three plots during the experimental period, we used mean values across all plots for each sampling date in addition to the individual measurements at each plot for correlation analyses.

Analyses

Fourier-transform infrared spectroscopy

We analyzed pure mineral mixtures and mineral mixtures loaded with ARE by Fourier-transform infrared (FTIR) spectroscopy in diffuse reflectance mode. We diluted the samples 1:10 with KBr, previously ground to powder and dried overnight at 105 °C. The sample and KBr powder were homogenized with a mortar and pestle, transferred into a sample cylinder and the top was leveled off (without pressure). We recorded 250 spectra per sample with the external DRIFT (diffuse reflectance infrared Fourier transform) module of a LUMOS infrared microscope (Bruker, Ettlingen, Germany) at a resolution of 4 cm^{-1} in the spectral range of 4000 to 600 cm^{-1}. The background was recorded against pure KBr. All spectra were normalized to the absorption band at 3650–3610 cm^{-1} of the OH-stretching vibration of octahedral illite sheets. In order to identify changes in the composition of organic matter present in the mineral mixtures during the field experiment, we subtracted the spectrum of the loaded mineral mixture at the start of the experiment from the respective sample spectra. We characterized the artificial exudates by subtracting the spectrum of the pure mineral mixture from the spectrum of the loaded mixture at the start of the experiment. Peak assignment was done according to Parikh et al. (2014). For comparison of FTIR spectra between the different treatments (high and low LUI) and between sampling dates, we used integrated absorption bands (main band between approximately 1032 and 990 cm^{-1}, smaller bands at 1075–1060 cm^{-1} (partially expressed as shoulder) and 942–912 cm^{-1}).

C, N, and ^{13}C

To determine organic C as well as $\delta^{13}C$ values, 4 g of soil and minerals was dried at 60 °C for 72 h and subsequently ground in a ball mill (Retsch GmbH & Co KG, Haan, Germany). Carbonates were removed by treating 100 mg of ground samples with 100 µl of 1 M HCl and drying for an additional 48 h at 60 °C. Samples were homogenized using mortar and pestle. Afterwards, 20–40 mg samples were measured with a coupled system consisting of an elemental analyzer (NA 1500, Carlo Erba, Milan, Italy) and an isotope ratio mass spectrometer (MAT 251, Thermo Finnigan, Bremen, Germany). The natural isotope abundance was described by the delta notation.

Extractable organic C (EOC) and extractable total N (ETN) were determined using the non-fumigated samples from the CFE analyses. Nitrogen content in minerals was near the detection limit and reliable values could not be obtained. Therefore, we only report the N content in the soil compartments. $\delta^{13}C$-EOC was determined as described for $\delta^{13}C_{mic}$. Calculation of % ARE-derived C in C_{org} and in EOC of the minerals was done using the following equation:

$$\%\text{ARE}-\text{derived C} = \frac{\delta^{13}C_{\text{minerals}} - \delta^{13}C_{\text{control soil}}}{\delta^{13}C_{\text{ARE}}} \times 100 \qquad (1)$$

To determine ARE-derived C for C_{org} and EOC in adjacent soils, $\delta^{13}C_{minerals}$ was replaced by $\delta^{13}C_{adjacent\ soil}$.

Microbial biomass C and N and resource use

Microbial biomass C (C_{mic}) and N (N_{mic}) were determined using the chloroform fumigation extraction (CFE) method according to Vance et al. (1987). Soil and minerals were thawed and 4 g field moist soil and 5 g field moist minerals were fumigated under vacuum with ethanol-free chloroform for 24 h. After removing the chloroform, soil samples were extracted with 32 ml and mineral samples with 20 ml of 0.025 M K_2SO_4 on a horizontal shaker at 250 rpm for 30 min. Samples were then centrifuged for 30 min at 4420 g to yield a clear supernatant (Marhan et al. 2010). To remove potentially present inorganic C, 60 µl of 1 M HCl was added to the supernatant of each sample. Organic C and total N were measured using a TOC-TNb Analyzer (Multi-N/C 2100S, Analytik Jena, Germany). It cannot be fully excluded that fine root–derived C contributed to chloroform-labile C in soil samples, even though all visible roots were removed prior to fumigation (Mueller et al. 1992). A second set of samples was extracted using the same approach, but without fumigation. Microbial C content was determined by the difference between C content of non-fumigated and C content of fumigated samples and calculated using a k_{EC} factor of 0.45 (Joergensen 1996). Microbial N content was calculated accordingly, but using a k_{EN} factor of 0.54 (Brookes et al. 1985). In minerals, N_{mic} was close to the detection limits, such that reliable values could not be obtained. Therefore, we report the microbial N content of the soil samples only.

$\delta^{13}C$ in C_{mic} was determined by evaporating 10 ml of fumigated and non-fumigated extracts at 60 °C in a rotatory evaporator (RVC 2-25, Martin Christ, Osterode am Harz, Germany) (Marhan et al. 2010). Afterwards, a minimum of 5 µg C per sample was weighed into tin capsules. Samples were analyzed with an elemental analyzer (Euro EA 3000, EuroVector, Milan, Italy) coupled with an isotope ratio mass spectrometer (IRMS, Delta Plus XP, Thermo Finnigan MAT, Bremen, Germany). The $\delta^{13}C$ values were expressed relative to Vienna Pee Dee belemnite (V-PDB). As a laboratory reference, acetanilide (C_8H_9NO, Merck, Germany) and glutamic acid (USGS-40 (IAEA, Austria; $\delta^{13}C$ -26.39 ± 0.04‰) were used. The following equation expresses the calculation of the $\delta^{13}C$ in C_{mic}:

$$\delta^{13}C_{mic} = \frac{cnf \times \delta nf - cf \times \delta f}{cnf - cf} \quad (2)$$

where *cnf* is the mass extracted organic C of the non-fumigated samples, *cf* the mass extracted organic C of the fumigated samples, and δnf and δf the respective $\delta^{13}C$ values. To calculate the relative proportion of ARE-derived C in C_{mic}, Eq. (1) was used.

Composition of main microbial groups and resource use

Phospholipid fatty acids (PLFAs) of Gram-positive bacteria (i15:0, a15:0, i16:0, i17:0), Gram-negative bacteria (cy17:0, cy19:0), and saprotrophic fungi (18:2ω6,9) were used as biomarkers to describe soil main microbial groups according to Ruess and Chamberlain (2010). There is still a debate as to whether or not some biomarkers common to a certain group of microorganisms might be also found in smaller amounts in other organisms. For this reason, we only selected PLFAs with a specific, internationally widely accepted biomarker function (Joergensen and Emmerling 2006). Extraction of PLFAs was performed after Frostegard et al. (1991). Briefly, field moist mineral and soil samples were thawed; 2 g soil and 20 g minerals were used for the extraction of neutral lipids and phospholipids. Alkaline methanolysis was used to transform PLFAs into fatty acid methyl esters (FAMEs), which were measured by gas chromatography (AutoSystem XL, PerkinElmer Inc., USA). For a detailed description of the method, see Kramer et al. (2013). The variable amounts of markers for the different microbial groups, as well as their varying content in single cells, are the reasons why we compare the differences between microbial groups only relatively.

The $\delta^{13}C$-PLFA values were determined as described by Müller et al. (2016) using a HP 6890 gas chromatograph (Agilent Inc., USA) coupled via combustion III interface (Thermo Finnigan, USA) to a Delta Plus XP mass spectrometer (Thermo Finnigan MAT, Germany). The $\delta^{13}C$ values were expressed relative to Vienna Pee Dee belemnite (V-PDB). For the correction of the $\delta^{13}C$ values, a mass balance equation was used following methanolysis ($\delta^{13}C$ value of methanol −40.23‰) according to Denef et al. (2007). Percent ARE-derived C in PLFAs was calculated using Eq. (1). To determine the proportion of ARE-derived C for PLFAs in the adjacent soil samples, $\delta^{13}C_{minerals}$ was replaced by $\delta^{13}C_{adjacent\ soil}$.

Mean absolute incorporation of ARE-derived C into the different microbial groups measured by PLFA was calculated by multiplying the percent ARE-derived C by the mass of C-atoms in the respective FAME. The content of ARE-derived C assimilated by each microbial group (i.e., Gram positive bacteria , Gram negative bacteria, and fungi), was calculated by summing the ARE-derived C of the respective individual FAMEs per microbial group (ng ARE-derived C g^{-1} soil DM).

Bacterial growth

Bacterial growth rate was determined using the methods of Bååth (1994) and Bååth et al. (2001). To measure the incorporation of ^3H-labeled leucine (Leu) into bacteria, 0.4 g of field moist sample (soil and minerals) was mixed with 5 ml purified water and centrifuged for 10 min at 1000 g. A subsample of 1.5 ml from the bacterial suspension was incubated for 2 h at 20 °C in the dark with a mixture of labeled and non-labeled Leu suspension, resulting in a final concentration of 275 nM Leu [3H]Leu (37 MBq ml^{-1} and 5.74 TBq $mmol^{-1}$, PerkinElmer, UK). Afterwards, bacterial growth was inhibited using 100% trichloroacetic acid and the unincorporated Leu was washed out through several washing steps (Bååth et al. 2001). The incorporated radioactive label was measured by liquid scintillation. Bacterial growth was represented by the incorporated 3H-Leu and was expressed as picomole Leu in extracted bacteria g^{-1} dry matter soil h^{-1}.

Fungal growth and biomass

Fungal growth was estimated using the method of Bååth et al. (2001) with adaptations by Rousk et al. (2009), which make use of the ability of fungi to incorporate acetate into ergosterol. For this, 0.4 g fresh soil or minerals were transferred into a 10 ml glass tube and a mixture of 20 µl 1-[^{14}C]acetic acid (sodium salt, 2.04 GBq $mmol^{-1}$, 7.4 MBq ml^{-1}, Perkin Elmer, USA) and unlabeled acetate was added, resulting in a final acetate concentration of 220 µM. Samples were incubated for 6 h at 20 °C in the dark. After phase separation and specific preparation steps, the quantity of ergosterol was measured using HPLC with a UV detector (282 nm) (LaChrom

Elite system with a Chromolith column (VWR-Hitachi)) and methanol (2 ml min^{-1}) as the mobile phase. The ergosterol fraction was separated with a fraction collector as described by Rousk and Bååth (2007). The incorporated ^{14}C acetate in ergosterol was measured using liquid scintillation. Ergosterol concentration corresponded to the fungal biomass, whereas the detected radioactivity, expressed as picomoles per gram soil per hour, represented fungal growth.

Molecular analyses of bacterial communities

The relative abundances of 16S rDNA amplicon sequence variants (V3 region) of bacterial taxa were determined by DNA analyses as described in Vieira et al. (2020). A Naïve Bayes classifier was used for taxonomic classification of representative sequences. Bacterial phyla were grouped into Gram-negative, Gram-positive, and unknown Gram status according to Rosenberg et al. (2013). High-throughput 16S rRNA gene amplicon sequencing enables bacterial community analysis at high taxonomic resolution, i.e., at sequence variant (SV) level. In contrast to PFLA, taxonomic entities are not determined as absolute quantities but rather in terms of relative abundance. Despite some limitations (Hugerth and Andersson 2017), amplicon sequencing has widely enabled significant insights into bacterial community composition (Delgado-Baquerizo et al. 2018; Thompson et al. 2017).

Statistical analysis

All statistical procedures were carried out in R version 3.6.0 (R Core Team 2019). We used linear mixed- effect models to evaluate the randomized split plot design of the study with the *lmer* function from the *lme4* package (Bates et al. 2015). The following general model structure was used for the soil samples, where we tested the effects of land-use intensity; soil sampling location, i.e., control or adjacent soil; and sampling time as independent variables:

$$y_{ijkl} = \mu + \alpha_i + \beta_j + \gamma_k + (\alpha\beta\gamma)_{ijk} + r_l + b_{jl} + c_{kl} + e_{ijkl} \quad (3)$$

For mineral samples and ^{13}C results of the adjacent soil, we tested the effects of land-use intensity and sampling time as independent variables by using the following general model structure:

$$y_{ijkl} = \mu + \alpha_i + \gamma_k + (\alpha\gamma)_{ik} + r_l + e_{ikl} \quad (4)$$

where y_{ijkl} is the value of the response variable for the ith level of LUI and jth soil sample location at the kth sampling time in lth site, μ is the general mean, α_i is the main effect of the ith level of LUI (abbreviated as "LUI" in the figures), β_j is the main effect of soil sampling location, γ_k is the main effect of the kth sampling time (abbreviated as "T" in the figures), $(\alpha\beta\gamma)_{ijk}$ is the interaction between the main effects, r_l is the random effect for site, b_{jl} is the random effect for the jth soil sampling location at the lth site, c_{kl} is the random effect for the kth sampling time at the lth site, and e_{ijkl} is the error. If differences between low and high LUI were not significant, we showed the mean values for all ten sites.

Differences in the composition of main microbial groups measured as PLFAs between adjacent soil, control soil, and minerals as well as between the different sampling dates within the mineral samples were analyzed by linear discriminant analysis using the *lda* function of the *MASS* package (Venables and Ripley 2002). The *ggord* package (Beck 2018) was used to calculate and display 95% confidence intervals based on weighted covariance matrices. Abundance effects that differed between sampling times or treatments were excluded by calculating the relative amounts of single microbial PLFAs as percent of the total number of PLFAs (n = 27) measured in a sample.

To express differences between the minerals and the control soil, we calculated the percentage of control soil values in minerals for any variable x as:

$$x_{\%\text{of control in minerals}} = \frac{x_{\text{minerals}}}{x_{\text{control}}} \times 100 \quad (5)$$

Results

Composition of mineral-associated organic matter

The differences in FTIR spectra between the pure mineral mixture and those loaded with ARE indicated that loading of the minerals was successful at the beginning of the experiment (Fig. 1a). These spectra corresponded to 54.7 μg of ARE-derived C (glucose and citric acid) associated with the pristine minerals. Nevertheless, the intensity of the ARE-derived bands of, for instance, carboxylic acid compounds had already declined after 2 weeks of exposure in the grassland soils, corresponding to one-third of the initially loaded ARE. A very broad absorption band (between 1150 and 885 cm^{-1}) of newly formed organic compounds, typically assigned to C-O-C and C-OH stretching vibrations of polysaccharides and polysaccharide-like compounds, was found in all of the exposed minerals as soon as 2 weeks after exposure (for an example, see Fig. 1b; for FTIR results of all sites, see Fig. S3). However, the peak areas of the integrated absorption bands did not change over time and were not affected by LUI.

Quantity of mineral-associated organic C fractions (C_{org}, EOC, C_{mic})

The C_{org} content in the minerals increased rapidly from an initial value of 281 μg C g^{-1} (sum of C_{org} in the original

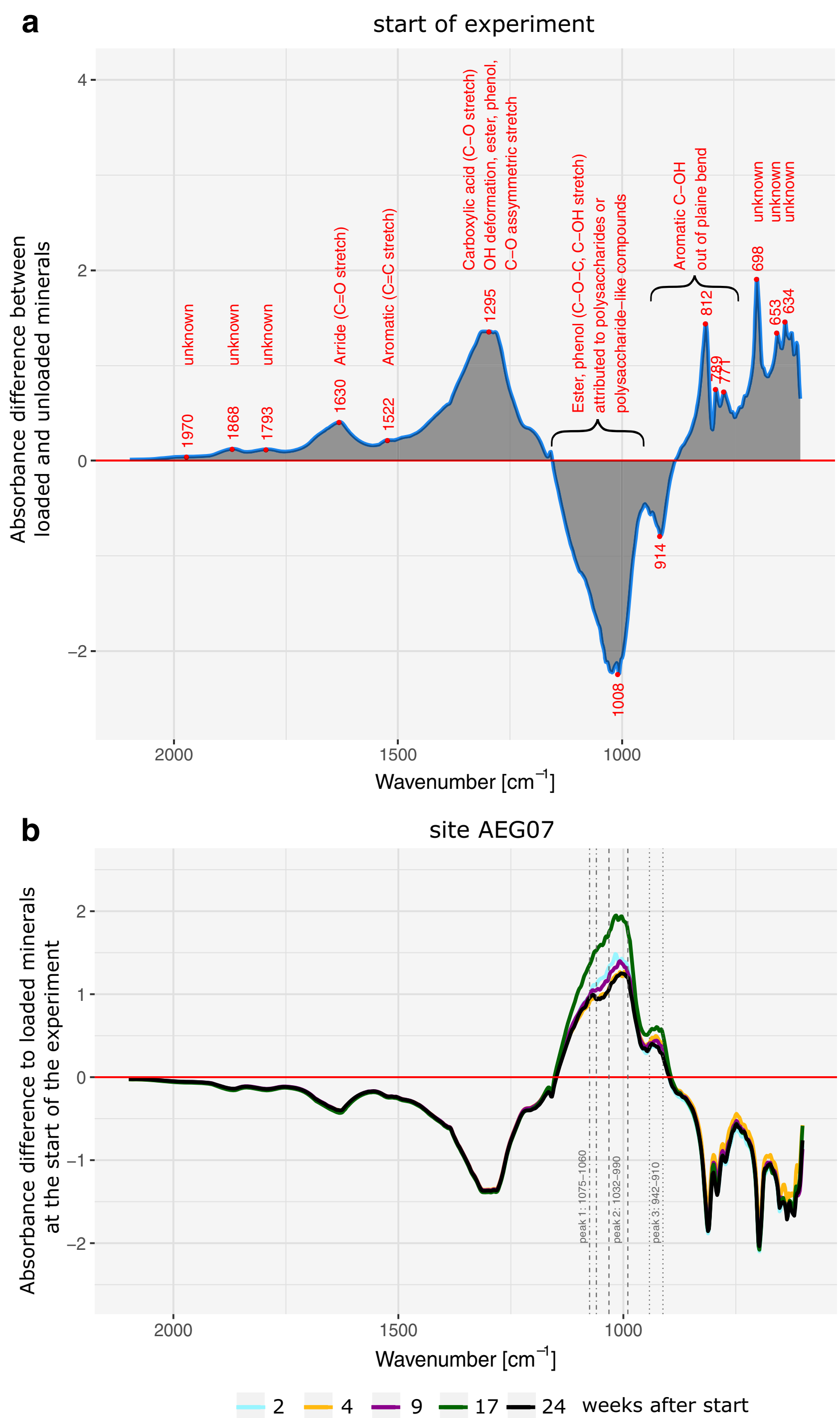

Fig. 1 Partial (2100–600 cm^{-1}) difference FTIR spectra for **a** mineral mixtures loaded with artificial root exudates relative to the unloaded mineral mixture before incorporation into the soil (= loaded–pure) with peak assignment according to Parikh et al. (2014) and **b** the buried mineral mixture at all sampling dates (two to 24 weeks after start) relative to the loaded mineral mixture at the start of the experiment, here as an example from site AEG07

minerals plus ARE-derived C) to about 900 μg g^{-1} during the first 2 weeks of exposure, decreased after 4 weeks of exposure, and increased subsequently up to 17 weeks of exposure (Fig. 2a). The content of extractable organic C (EOC) decreased until week 4, then increased, reaching the highest values after 24 weeks of exposure in the grassland soils (Fig. 2a). When related to C_{org}, EOC content also increased over time (T: $F_{4,\ 29}$ = 31.14, p < 0.001) (Table S2). Microbial biomass C (C_{mic}) steeply increased to week 4, more weakly increased to week 17, then decreased slightly (Fig. 2a).

ARE-derived C in C_{org} strongly decreased from an initial value of 54.7 μg g^{-1} to on average 17.9 μg g^{-1} (reduction by 67%) after 2 weeks of exposure and decreased steadily thereafter until 24 weeks (Fig. 2b). The relative amount of ARE-derived C in C_{org} also significantly decreased between the start of the experiment and 24 weeks of exposure, from 2.1% (SD ±

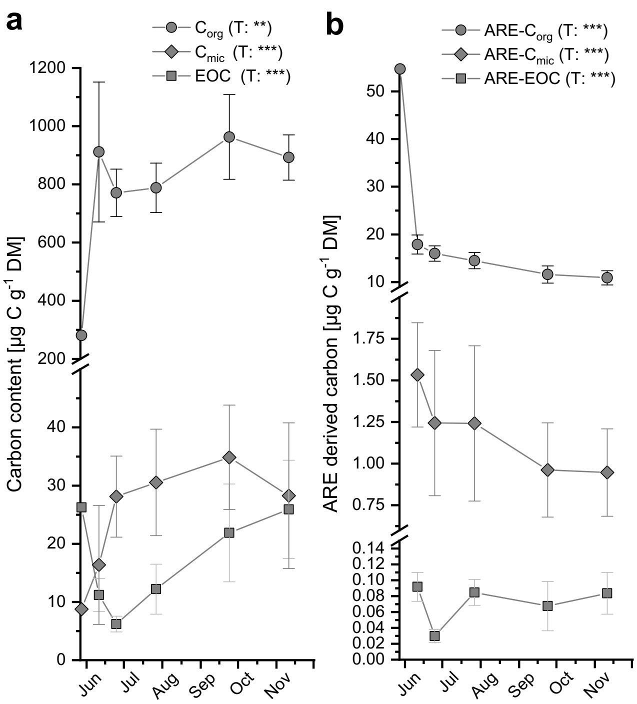

Fig. 2 **a** Carbon content in soil organic C (C_{org}), extractable organic C (EOC), and microbial biomass (C_{mic}) per g dry matter (DM) of mineral mixtures and **b** content of artificial root exudate (ARE)–derived C in C_{org}, EOC, and C_{mic}. No LUI effects were found; therefore, $n = 10$, mean ± SD. Significance of the sampling time (T) effect is indicated by $^{***}p < 0.001$ and $^{**}p = 0.001 < p < 0.01$

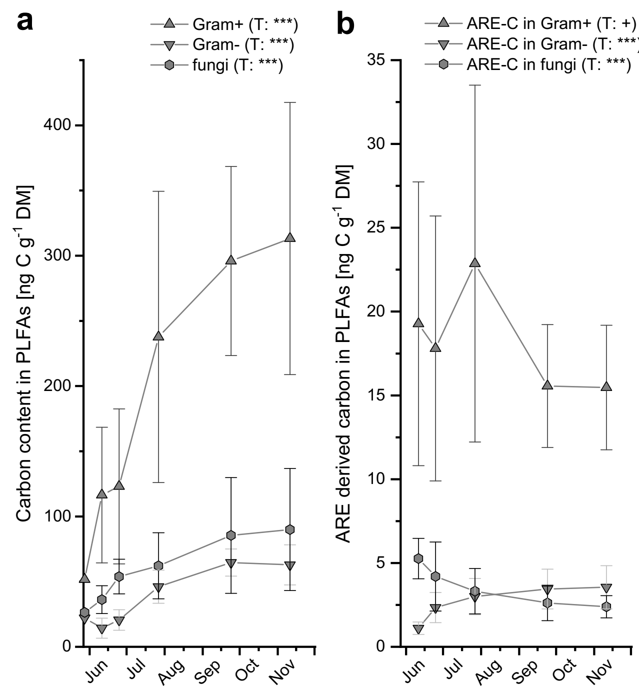

Fig. 3 **a** Content of fatty acid methyl esters (FAMEs) from phospholipid fatty acids (PLFAs) for Gram-positive (Gram+) bacteria, Gram-negative (Gram−) bacteria, and saprotrophic fungi (fungi) ($n = 10$, mean ± SD). **b** Content of artificial root exudate (ARE)–derived C in PLFA FAMEs of Gram-positive bacteria, Gram-negative bacteria, and fungi ($n = 10$, mean ± SD) in minerals. Significance of the sampling time (T) effect is indicated by $^{***}p < 0.001$ and $^{+}0.05 < p < 0.1$

0.5%) to 1.2% (SD ± 0.2%) (Table S2, S3). The content of ARE-derived C in EOC fluctuated between the sampling dates but did not show a trend over time (Fig. 2b). In contrast, the relative amount of ARE-derived C in EOC decreased by half over time and was higher in minerals buried in low than in high LUI grassland sites (Table S2, S3). The quantity of ARE-derived C in C_{mic} was highest after 2 weeks and steadily decreased afterwards (Fig. 2b), representing relative contributions of ARE-derived C to C_{mic} of 12.2% after 2 weeks and to less than 5.0% at the following samplings (Table S2). LUI had neither an effect on C_{org} nor on the ARE-derived C in the C_{org} and C_{mic} pool.

While bacterial growth rates showed a general increase over time, fungal growth rates fluctuated and did not show a temporal trend, neither did ergosterol content (Table S2, S3).

The abundances of Gram-positive and Gram-negative bacteria as well as that of fungi significantly increased over time (Fig. 3a). The increase in bacterial abundance was most pronounced between four and 9 weeks of exposure, whereas the strongest increase in fungal abundance occurred earlier, between two and 4 weeks. While Gram-positive bacterial abundance further increased throughout 24 weeks of exposure, Gram-negative bacterial abundance reached a plateau from 17 weeks on. The increase in fungal abundance was less steep than the increase in Gram-positive bacterial abundance, but comparable to that of Gram-negative bacteria, considering the entire experimental period. Discriminant function analysis based on single PLFAs across all sampling time points indicated a shift within the microbial communities from the first to the last sampling, even though the main microbial groups established did not significantly differ from each other (Fig. S4a and Table S4a).

The absolute (Fig. 3b) as well as the relative (Table S2) amount of ARE-derived C decreased over time slightly in Gram-positive bacteria but was more pronounced in saprotrophic fungi. In Gram-negative bacteria, the relative amount of ARE-derived C also decreased from week four on, though less pronounced than in the other two microbial groups (Table S2); together with their increase in abundance, this led to increasing absolute amounts of ARE-derived C in Gram-negative bacteria over time (Fig. 3b). The decrease in the relative amount of ARE-derived C was steepest in fungi; in this microbial group alone, LUI had an effect. A generally higher proportion of ARE-derived C was detected in fungi inhabiting minerals buried in low than in high LUI soils (Table S2).

As Gram-negative bacteria behaved differently in comparison to the other microbial groups, we took a closer look using next-generation sequencing data. The bacterial phyla from Vieira et al. (2020) were assigned to Gram-negative, Gram-positive, or unknown Gram reaction depending on the predominant properties of each phylum (Rosenberg et al. 2013). By combining this information with Spearman correlations between Gram-negative PLFA abundance and relative abundances of the detected phyla, we found that the total relative sequence abundance of Gram-negative bacteria was positively correlated with Gram-negative PLFAs ($r = 0.31$, $p = 0.028$). The Gram-negative bacteria in the mineral mixture consisted mainly of *Proteobacteria*, *Bacteroidetes*, *Verrucomicrobia*, *Acidobacteria*, *Planctomycetes*, *Chloroflexi*, *Gemmatimonadetes*, and *Armatimonadetes*. Of these, *Proteobacteria* and *Bacteroidetes* were the highest in relative abundances, but were not positively correlated to Gram-negative PLFA abundance (Fig. S5a). Instead, the relative abundance of bacterial phyla *Verrucomicrobia*, *Planctomycetes*, *Gemmatimonadetes*, *Armatimonadetes*, and *Chloroflexi* was positively correlated with Gram-negative PLFA abundances. The relative abundance of the phyla *Cyanobacteria*, *Tenericutes*, and *Poribacteria* was negatively correlated with the abundance of Gram-negative PLFAs as well, but had very low relative abundances and are therefore not further considered.

Of the Gram-positive bacterial phyla, *Actinobacteria*, *Firmicutes*, and *Deinococcus-Thermus* were detected. Of these, the *Actinobacteria* were most abundant, but not correlated with Gram-positive PLFA abundance, while the relative abundances of *Firmicutes* and *Deinococcus-Thermus* were negatively correlated with Gram-positive PLFA abundances (Fig. S5b).

Comparison of C_{org}, EOC, C_{mic}, and PLFAs between minerals and surrounding soil

In general, colonization of the mineral mixture newly introduced into the grassland soil was slow. C_{mic} reached on average 2.3% (SD ± 0.7%) of the control soil after 17 weeks of exposure before it dropped again to 1.9% (SD ± 1%) after 24 weeks (Table S2). Regarding the different microbial groups, saprotrophic fungi reached higher colonization levels than the two bacterial groups (Fig. 4). While bacteria did not reach levels higher than on average 1.7% (SD ± 0.5%) of the control soil even after 24 weeks of exposure, saprotrophic fungi made up on average 1.6% (SD ± 0.7%) of the control soil after only 2 weeks of exposure and reached levels of on average 5.2% (SD ± 2.9%) of the control soil after 24 weeks. Fungi were additionally affected by LUI with on average 1.2-fold higher fungal abundance in high vs. low LUI sites (LUI: $F_{1,\ 8} = 11.05$, $p = 0.01$)

Discriminant function analysis of the composition of main microbial groups in soil and mineral samples indicated a significant difference between the soil samples and minerals after 24 weeks of exposure. This difference in the composition of main microbial groups was mainly attributed to the Gram-

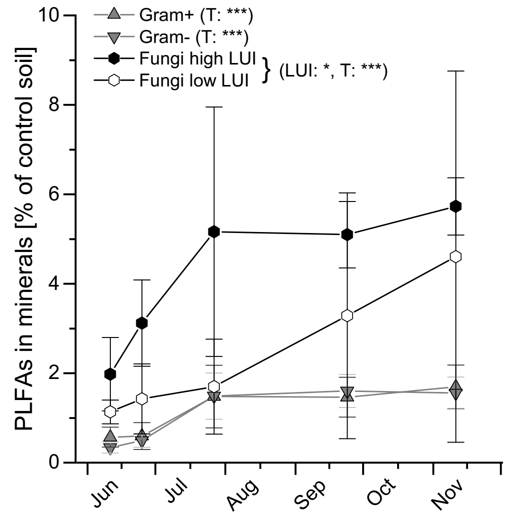

Fig. 4 Percent of phospholipid fatty acids (PLFAs) measured in the mineral mixtures as compared to control soil values for Gram-positive (Gram+) bacteria, Gram-negative (Gram−) bacteria, and fungi (fungi) at the five sampling dates ($n = 10$, except for fungi high and low LUI $n = 5$, mean ± SD). Significance of the effects of land-use intensity effect (LUI) and sampling time (*T*) is indicated by ***$p < 0.001$ and *$0.01 < p < 0.05$

positive PLFA i17:0 followed by the Gram-negative PLFA cy17:0 (Fig. S4b and Table S4b).

C_{mic} as a percent of C_{org} was somewhat higher in the minerals compared to the control soil, exceeding that of the control soil by a factor of up to 2.3 (Fig. S6). The same was observed for bacterial growth rates, with mean values in minerals above 100% of the control soil after 17 and 24 weeks of exposure (165%, SD ± 213% and 124% SD ±95%, respectively) (Fig. S7). In contrast, fungal growth rates were on average always lower in the minerals compared to the control soil (95% ± SD 77%) even though they peaked at up to 270% of the control soil at a single site after 9 weeks of exposure (Fig. S7).

The soil sampled 1 cm above and below the mineral container (adjacent soil) was slightly different from the control bulk soil due to its close contact to the mineral containers. Both C_{mic} and N_{mic} were higher in the adjacent soil than in the control soil (Table S2, S3). The percent C_{mic} of C_{org} was also higher in the adjacent soil than in the control soil, while the percent EOC of C_{org} was lower (Table S2, S3). With respect to LUI effects, C_{mic} and the percent C_{mic} of C_{org} were both higher in high LUI compared to low LUI sites and in the control as well as in the adjacent soil (Table S2).

In the control and adjacent soil, both fungal PLFA abundance and the PLFA fungi to bacteria ratio were higher in low than in high LUI sites. We also detected higher bacterial growth rates in low LUI sites (LUI: $F_{1,\ 8} = 9.48$, $p = 0.015$), while fungal growth was not significantly different between high and low LUI (Table S2).

ARE-derived C was transported from the mineral containers into the adjacent soil, as $\delta^{13}C_{mic}$ and δ^{13}C-EOC values were significantly higher in the adjacent soil compared to the control soil (Table S2). Similar to the decrease in ARE-derived C in C_{mic} in the minerals, the content of ARE-derived C also decreased in C_{mic} in the adjacent soil (Fig. S8).

Discussion

Quantity and composition of mineral-associated C

The exposure of mineral containers loaded with labeled glucose and citric acid in different grassland sites for 24 weeks made it possible to follow changes in quality and quantity of mineral-associated C as well as microbial colonization and C use by different groups of microorganisms.

Using FTIR spectra, we demonstrated that the composition of mineral-associated C changed within the first 2 weeks of exposure of the mineral containers, but remained constant during the following exposure time. Polysaccharides and polysaccharide-like compounds initially accumulated due to the presence of added ARE (Fig. 1), which can be explained by rapid microbial use of the original loaded ARE. These compounds declined by 67 percent after 2 weeks (Fig. 2b) while in the same period, the content of mineral-associated C_{org} increased (Fig. 2a). When attaching to mineral surfaces, microorganisms utilize biofilms/extracellular polymeric substances (EPS; Cuadros 2017), which dominantly consist of polysaccharides. Accordingly, we detected FTIR absorption bands typical of polysaccharides 2 weeks after the mineral mixtures had been exposed in soil. At near-neutral pH, bacterial cell walls, and EPS have a net negative charge (Cuadros 2017). Thus, they are attracted by positively charged goethite. Negatively charged phyllosilicate surfaces form bridges to cell walls/EPS via divalent cations (Cuadros 2017). Particularly, Ca ions promote EPS adsorption on minerals, rather than monovalent cations (Cao et al. 2011). Consequently, cation bridging is a very likely process involved in the colonization of illite surfaces in our experiment, given the composition of exchangeable cations mentioned before. Neither the charge properties nor the chemical status of the minerals used in our study gives evidence of hostile conditions regarding microbial colonization. In addition, heavy rain events shortly before the first sampling (Fig. S1) probably transported dissolved organic C from the adjacent soil into the mineralosphere. Therefore, we assume that different substrate sources, ARE-derived glucose and citric acid, microbially processed ARE, as well as soil-derived polysaccharides, polysaccharide-like compounds, and other complex C compounds were used by microorganisms in the mineralosphere over the longer exposure time of the mineral containers. Significantly lower relative content of ARE-derived EOC under high land-use intensity indicated that more external C reached the mineralosphere at high LUI sites, which are characterized by higher C_{org} contents, than low LUI sites.

Mineral colonization and resource use

The mineralosphere as habitat for soil microorganisms developed swiftly on the exposed ARE-loaded pristine minerals (Fig. 2a). This is in line with the study by Ma et al. (2017) who showed that microcolonies formed rapidly on different soil minerals. In a laboratory study, Whitman et al. (2018) found higher total DNA concentrations in the mineralosphere than in the surrounding soil. In our study, subsequent colonization by soil microorganisms after 4 weeks of exposure was slow and reached a maximal C_{mic} content after 17 weeks. Considering the abundance of bacterial and fungal PLFAs in the mineralosphere (Fig. 3), our findings are in line with previous studies (Kandeler et al. 2019; Vieira et al. 2020), which found faster colonization of the mineralosphere by fungi than by bacteria, thus supporting our second hypothesis. Since the study of Kandeler et al. (2019) used the same mineral container composition as did the current study, but with root litter as the complex C-source, the dominance of fungi during initial colonization of mineralization seems to be independent of resource quality. The importance of the physical environment's impact on microorganisms with different life history strategies was also illustrated by Tecon and Or (2017) as well as Seaton et al. (2020). Due to their hyphal growth, fungi can actively grow toward new food sources (Fukasawa et al. 2019), while bacteria are strongly limited in individual movement at the centimeter scale (Abu-Ashour et al. 1998). How bacterial cells are transported into the mineralosphere is still under discussion. The following mechanisms are possible: active movement of motile bacteria (growth, swimming, swarming, and twitching motility), as well as passive water transport by diffusion and convection (Yang and van Elsas 2018). Fungal hyphae may also be facilitators of short- and long-distance migration of bacteria through soil, with implications for the bacterial occupancy of novel ecological niches like the mineralosphere (Yang and van Elsas 2018). In addition, fungi can reallocate water, nutrients, and C resources through their hyphal network (Cairney 1992; Simonin et al. 2012; Whiteside et al. 2019). Recent results have shown that fungal hyphal networks can bridge different substrate islands over distances of 27 mm even under low moisture conditions, indicating that these bridges may act as nutrient highways under drought conditions (Bhattacharjee et al. 2020). These mechanisms may also explain why fungi under high LUI colonized the mineralosphere to a greater extent than fungi under low LUI. Fungal mycelia likely bridged the external bulk soil particles and the mineralosphere, transporting more external C in their hyphae to the mineralosphere from high LUI than from low LUI sites. Since soil N contents tended to be higher in high than low LUI soils (Table S1), we speculate that fungi may also transport soil-derived N into the mineralosphere. This transport mechanism was also identified by Frey et al. (2000, 2003) between the detritusphere and the upper soil layers.

In general, our study could not prove that bacteria use fungal highways to gain rapid access to the substrate (Simon et al. 2017) and consequently did not outcompete their fungal carrier locally. The low importance of fungal highways is also supported by the fact that we could not detect a high relative abundance of Burkholderia that are well-known as potentially associated migrating bacteria in soils (Simon et al. 2015, 2017). In our study, bacteria have to solely rely on the nutrients and resources available in their immediate vicinity (Purcell 1977).

The data on colonization of minerals by Gram-positive and Gram-negative bacteria (using PLFA data) were compared with 16S rRNA data previously analyzed by Vieira et al. (2020). In general, we found a positive correlation between Gram-negative PLFA abundances and relative abundance of sequence variants. However, this could not be verified for the high abundant, mostly Gram-negative *Proteobacteria* and *Bacteroidetes*. Since our PLFA analysis includes only two fatty acids as indicators for Gram-negative bacteria, it is questionable whether these two phyla contain the two indicator PLFAs in a sufficient amount (Zelles 1997). In addition, it is well known that the PLFA composition can vary with the physiological state of the bacteria (Zelles 1999). Regarding Gram-positive bacteria, there is evidence of a very strong response of two sequence variants belonging to the family Micrococcaceae (Gram-positive), particularly in the early stages of mineral colonization, which can make up 37.3% of all detected sequence variants (Vieira et al. 2020). Therefore, we do not believe this to be due to the lack of detection of suitable PLFA markers, rather due to Gram-negative bacteria being outcompeted by Gram-positive bacteria, particularly by these two Micrococcaceae sequence variants. One possible reason for the strong response of the two Micrococcaceae sequence variants may be related to the capabilities of members of this family to adhere and dissolve minerals through the formation of complexing agents and a decrease in pH (Vieira et al. 2020).

Whereas all microbial indicators (C_{mic}, Gram-positive, Gram-negative bacteria, and fungi) increased in abundance over time, substrate incorporation of ARE-derived C peaked only in Gram-positive bacteria and fungi at the beginning of the exposure period. This immediate use of the provided resource was expected and supports the results of Paterson et al. (2008), who detected C-derived from soluble and insoluble plant tissues in soil respiration after only 2 h. For both Gram-positive bacteria and fungi, ARE-derived C in PLFAs decreased over time, indicating that both bacteria and fungi relied on ARE as a substrate at the beginning of the experiment, but made use of alternative C resource derived from outside the mineralosphere later in the season, supporting our third hypothesis.

Besides microbial respiration and assimilation of ARE in the mineralosphere, small amounts of ARE were found in the adjacent soil where they were assimilated by soil microorganisms (Fig. S8). ARE-derived C could either be transported as DOC from a mineral container into adjacent soil or by microbially mediated transport (e.g., through the hyphal networks bridging the mineral containers with the adjacent soil).

We found one exception to the general trend of decreasing ARE-derived C in microorganisms during time of exposure. The absolute amount of ARE-derived C increased in Gram-negative bacteria over time. The most likely explanation is that this group of microorganisms obtained their C from cross-feeding on fungal and Gram-positive bacteria (Müller et al. 2016, 2017; Smith et al. 2019). Nevertheless, we also speculate that Gram-negative bacteria are less competitive for this resource than Gram-positive bacteria and fungi and/or that they have lower turnover and uptake rates of newly available C than the other groups of microorganisms. Consequently, we dug deeper into the taxonomy of Gram-negative bacteria. We found that the relative abundances of the bacterial phyla *Verrucomicrobia*, *Planctomycetes*, *Gemmatimonadetes* and *Armatimonadetes*, previously linked mainly with oligotrophy (Ditterich et al. 2016; Lee et al. 2014; Uksa et al. 2015), and that of *Chloroflexi* (Hanada 2014) were positively correlated with Gram-negative PLFA abundances. Oligotrophic bacteria are considered able to process more complex C sources (Fierer et al. 2007). Therefore, the delayed assimilation of ARE into Gram-negative bacteria may have been due to their ability to feed on complex substrates derived from Gram-positive bacteria and fungi.

Interaction of the mineralosphere with their environment

In agreement with earlier studies (Kandeler et al. 2019; Vieira et al. 2020), the abundance of microorganisms in the new habitat (mineralosphere) is much smaller than in the bulk soil in the short and long term (6–31 months). Discussing this result in a broader context, we must consider the mode of exposure of the mineral containers. The prerequisite for exposure of mineral containers was the use of a mesh (< 50 μm) which isolated the mineralosphere from the surrounding soil. This mesh may also have served as a barrier to soil animals with a body size of > 50 μm. Although we do not have any data on soil fauna, the mesh of the mineral containers would have prevented the migration of soil animals larger than 50 μm into the mineralosphere. The exclusion of larger soil animals also prevented any bioturbation in the mineral containers that otherwise could have led to an accelerated mixing of organic substrates. The food web in the mineralosphere was less complex than in either soil fraction (adjacent and control soil). For example, microarthropods could not feed on fungal hyphae in the mineralosphere; this, in turn, could have modified C cycling (Crotty and Adl 2019; Pausch et al. 2015, 2018). It was beyond the scope of this paper to additionally explore the importance of trophic interactions and soil physics (such as particle size distribution, pore geometry, connectivity, and hydration status) to microbial colonization and C use in the mineralosphere (Seaton et al. 2020). Nevertheless, our approach can be extended to study the importance of physical structure of minerals and soils to trophic interactions in the mineralosphere (Erktan et al. 2020).

Conclusion

The present study focused on colonization and functioning of soil microorganisms in the mineralosphere of different grassland soils. We found that the three microbial groups colonized the pristine minerals and used the ARE to a different extent. Whereas fungi and Gram-positive bacteria used the artificial root exudates immediately after exposure in the soil, Gram-negative bacteria seemed to have been secondary users and probably relied more on cross-feeding on ARE-derived C formerly assimilated by fungi and Gram-positive bacteria. Based on abundance data (C_{mic}, PLFAs, sequencing) and physiological properties of bacteria and fungi (growth rates and C assimilation), the mineralosphere and the bulk soil are two distinct habitats (Fig. S4). Over longer time periods, microbial populations and element cycling in the mineralosphere will become more and more similar to the bulk soil. Nevertheless, more research is needed investigating the colonization of minerals over longer time periods. Further, the effect of the type of the minerals on the microbial colonization and organic matter turnover needs more attention.

Supplementary Information The online version contains supplementary material available at https://doi.org/10.1007/s00374-021-01551-7.

Acknowledgements We thank the managers of the three exploratories, Kirsten Reichel-Jung, Katrin Lorenzen, Martin Gorke, and Miriam Teuscher, and all former managers for their work in maintaining the plot and project infrastructure; Christiane Fischer and Jule Mangels for giving support through the central office; Michael Owonibi for managing the central database, the instrumentation, and remote sensing team of Thomas Nauss for providing soil temperature and moisture data; and Markus Fischer, Eduard Linsenmair, Dominik Hessenmöller, Daniel Prati, Ingo Schöning, François Buscot, Ernst-Detlef Schulze, Wolfgang W. Weisser, and the late Elisabeth Kalko for their role in setting up the Biodiversity Exploratories project. We also thank Kathleen Regan for English corrections as well as Doreen Berner, Karolin Müller, Hanna Frick, and Miriam Kempe for field and laboratory support.

Author contribution Ellen Kandeler, Sven Marhan, and Runa S. Boeddinghaus wrote the manuscript. Runa S. Boeddinghaus and Sven Marhan performed data analyses. Aurelia Gebala and Heike Haslwimmer conducted the experiment and performed most laboratory analyses. Ellen Kandeler, Sven Marhan, and Thilo Rennert coordinated and designed the study. Thilo Rennert was responsible for FTIR measurements. Johannes Rousk and Margarida Soares supervised growth rate analyses. Selma Vieira, Johannes Sikorski, and Jörg Overmann provided molecular data. All authors read and revised the manuscript.

Funding Open Access funding enabled and organized by Projekt DEAL. The work of Aurelia Gebala and Runa S. Boeddinghaus has been funded by the Deutsche Forschungsgemeinschaft (DFG) Priority Program 1374 "Infrastructure-Biodiversity-Exploratories" (KA1590/8-3, KA 1590/8-4). Fieldwork permits were issued by the responsible state environmental office of Baden-Württemberg.

Data availability The datasets generated during the current study are available at the ENA repository (https://www.ebi.ac.uk/ena/browser/view/PRJEB32280) and at BExIS (https://www.bexis.uni-jena.de/PublicData/About.aspx; with data IDs 19007, 24786, 26148, 26149 and 26150).

Declarations

Conflict of interest The authors declare no conflict of interest.

References

Abu-Ashour J, Joy DM, Lee H, Whiteley HR, Zelin S (1998) Movement of bacteria in unsaturated soil columns with macropores. Trans ASABE 41:1043–1050

Ahmed E, Holmström SJM (2015) Micro-mineral interactions: the impact of surface attachment on mineral weathering and element selectivity by microorganisms. Chem Geol 403:13–23

Bååth E (1994) Measurement of protein synthesis by soil bacterial assemblages with the leucine incorporation technique. Biol Fertil Soils 17:147–153

Bååth E, Pettersson M, Söderberg KH (2001) Adaptation of a rapid and economical microcentrifugation method to measure thymidine and leucine incorporation by soil bacteria. Soil Biol Biochem 33:1571–1574

Babin D, Ding GC, Pronk GJ, Heister K, Kögel-Knabner I, Smalla K (2013) Metal oxides, clay minerals and charcoal determine the composition of microbial communities in matured artificial soils and their response to phenanthrene. FEMS Microbiol Ecol 86:3–14

Babin D, Vogel C, Zühlke S, Schloter M, Pronk GJ, Heister K, Spiteller M, Kögel-Knabner I, Smalla K (2014) Soil mineral composition matters: response of microbial communities to phenanthrene and plant litter addition in long-term matured artificial soils. PLoS One 9:e106865

Bates D, Maechler M, Bolker B, Walker S (2015) Fitting linear mixed-effects models using lme4. J Stat Softw 67:1–48

Beck MW (2018) ggord: ordination plots with ggplot2. R package version 113

Berns AE, Philipp H, Narres HD, Burauel P, Vereecken H, Tappe W (2008) Effect of gamma-sterilization and autoclaving on soil organic matter structure as studied by solid state NMR, UV and fluorescence spectroscopy. Eur J Soil Sci 59:540–550

Bhattacharjee A, Velickovic D, Wietsma TW, Bell SL, Jansson JK, Hofmockel KS, Anderton CR (2020) Visualizing microbial community dynamics via a controllable soil environment. mSystems 5: e00645–e00619

Blüthgen N, Dormann CF, Prati D, Klaus VH, Kleinebecker T, Hölzel N, Alt F, Boch S, Gockel S, Hemp A, Müller J, Nieschulze J, Renner SC, Schöning I, Schumacher U, Socher SA, Wells K, Birkhofer K, Buscot F, Oelmann Y, Rothenwöhrer C, Scherber C, Tscharntke T, Weiner CN, Fischer M, Kalko EKV, Linsenmair KE, Schulze ED, Weisser WW (2012) A quantitative index of land-use intensity in grasslands: Integrating mowing, grazing and fertilization. Basic Appl Ecol 13:207–220

Boeddinghaus RS, Marhan S, Berner D, Boch S, Fischer M, Hölzel N, Kattge J, Klaus VH, Kleinebecker T, Oelmann Y, Prati D, Schäfer D, Schöning I, Schrumpf M, Sorkau E, Kandeler E, Manning P (2019) Plant functional trait shifts explain concurrent changes in the structure and function of grassland soil microbial communities. J Ecol 107:2197–2210

Bray RH, Kurtz LT (1945) Determination of total, organic, and available forms of phosphorus in soils. Soil Sci 59:39–46

Brookes PC, Kragt JF, Powlson DS, Jenkinson DS (1985) Chloroform fumigation and the release of soil nitrogen: the effects of fumigation time and temperature. Soil Biol Biochem 17:831–835

Cairney JWG (1992) Translocation of solutes in ectomycorrhizal and saprotrophic rhizomorphs. Mycol Res 96:135–141

Cao Y, Wei X, Cai P, Huang Q, Rong X, Liang W (2011) Preferential adsorption of extracellular polymeric substances from bacteria on clay minerals and iron oxide B: Biointerfaces. Colloid Surface 83: 122–127

Chenu C, Stotzky G (2002) Interactions between microorganisms and soil particles: an overview. In: Huang PM, Bollag JM, Senesi N (eds) Interaction between soil particles and microorganisms. John Wiley & Sons, Chichester, pp 4–29

Crotty FV, Adl SM (2019) Competition and predation in soil fungivorous microarthropods using stable isotope ratio mass spectrometry. Front Microbiol 10:1274

Cuadros J (2017) Clay minerals interaction with microorganisms: a review. Clay Miner 52:235–261

Delgado-Baquerizo M, Oliverio AM, Brewer TE, Benavent-González A, Eldridge DJ, Bardgett RD, Maestre FT, Singh BK, Fierer N (2018) A global atlas of the dominant bacteria found in soil. Science 359: 320–325

Denef K, Bubenheim H, Lenhart K, Vermeulen J, Van Cleemput O, Boeckx P, Müller C (2007) Community shifts and carbon translocation within metabolically-active rhizosphere microorganisms in grasslands under elevated CO_2. Biogeosci 4:769–779

Ditterich F, Poll C, Pronk GJ, Heister K, Chandran A, Rennert T, Kögel-Knabner I, Kandeler E (2016) Succession of soil microbial communities and enzyme activities in artificial soils. Pedobiologia 59:93–104

Eilers KG, Lauber CL, Knight R, Fierer N (2010) Shifts in bacterial community structure associated with inputs of low molecular weight carbon compounds to soil. Soil Biol Biochem 42:896–903

Erktan A, Or D, Scheu D (2020) The physical structure of soil: determinant and consequence of trophic interactions. Soil Biol Biochem 148:107876

Fierer N, Bradford MA, Jackson RB (2007) Toward an ecological classification of soil bacteria. Ecol 88:1354–1364

Fischer M, Bossdorf O, Gockel S, Hänsel F, Hemp A, Hessenmöller D, Korte G, Nieschulze J, Pfeiffer S, Prati D, Renner S, Schöning I, Schumacher U, Wells K, Buscot F, Kalko EKV, Linsenmair KE, Schulze E-D, Weisser WW (2010) Implementing large-scale and long-term functional biodiversity research: the Biodiversity Exploratories. Basic Appl Ecol 11:473–485

Frey SD, Elliott ET, Paustian K, Peterson GA (2000) Fungal translocation as a mechanism for soil nitrogen inputs to surface residue decomposition in a no-tillage agroecosystem. Soil Biol Biochem 32:689–698

Frey SD, Six J, Elliott ET (2003) Reciprocal transfer of carbon and nitrogen by decomposer fungi at the soil–litter interface. Soil Biol Biochem 35:1001–1004

Frostegard A, Tunlid A, Bååth E (1991) Microbial biomass measured as total lipid phosphate in soils of different organic content. J Microbiol Met 14:151–163

Fukasawa Y, Savoury M, Boddy L (2019) Ecological memory and relocation decisions in fungal mycelial networks: responses to quantity and location of new resources. ISME J 14:380–388

Grayston SJ, Vaughan D, Jones D (1997) Rhizosphere carbon flow in trees, in comparison with annual plants: the importance of root exudation and its impact on microbial activity and nutrient availability. Appl Soil Ecol 5:29–56

Hagenberg D, Thelin G, Wallander H (2003) The production of ectomycorrhizal mycelium in forests: relation between forest nutrient status and local mineral sources. Plant Soil 252:279–290

Hanada S (2014) The phylum Chloroflexi, the family Chloroflexaceae, and the related phototrophic families Oscillochloridaceae and Roseiflexaceae. In: Rosenberg, E, DeLong, EF, Lory, S, Stackebrandt, E, Thompson, F (eds) The prokaryotes: Other major lineages of bacteria and the archaea. Springer, Berlin, pp 515–532

Hemkemeyer M, Pronk GJ, Heister K, Kögel-Knabner I, Martens R, Tebbe CC (2014) Artificial soil studies reveal domain-specific preferences of microorganisms for the colonisation of different soil minerals and particle size fractions. FEMS Microbiol Ecol 90:770–782

Hugerth LW, Andersson AF (2017) Analysing microbial community composition through amplicon sequencing: from sampling to hypothesis testing. Front Microbiol 8:22

Hünninghaus M, Dibbern D, Kramer S, Koller R, Pausch J, Urich T, Kandeler E, Bonkowski M, Lueders T (2019) Disentangling carbon flow across microbial kingdoms in the rhizosphere of maize. Soil Biol Biochem 134:122–130

IUSS Working Group WRB (2015) World Reference Base for Soil Resources 2014, update 2015. International soil classification system for naming soils and creating legends for soil maps. In World Soil Resources Reports. Rome: FAO

Joergensen RG (1996) The fumigation-extraction method to estimate soil microbial biomass: Calibration of the kEC value. Soil Biol Biochem 28:25–31

Joergensen RG, Emmerling C (2006) Methods for evaluating human impact on soil microorganisms based on their activity, biomass, and diversity in agricultural soils. J Plant Sci and Soil Sci 169: 295–309

Johnson-Maynard JL, Strawn DG (2016) Linking physical and biogeochemical properties and processes in the drilosphere. Soil Sci 181: 126–132

Kallenbach CM, Frey SD, Grandy AS (2016) Direct evidence for microbial-derived soil organic matter formation and its ecophysiological controls. Nat Commun 7:13630

Kandeler E, Gebala A, Boeddinghaus RS, Müller K, Rennert T, Soares M, Rousk J, Marhan S (2019) The mineralosphere – succession and physiology of bacteria and fungi colonising pristine minerals in grassland soils under different land-use intensities. Soil Biol Biochem 136:107534

Kramer S, Dibbern D, Moll J, Huenninghaus M, Koller R, Krueger D, Marhan S, Urich T, Wubet T, Bonkowski M, Buscot F, Lueders T, Kandeler E (2016) Resource partitioning between bacteria, fungi, and protists in the detritusphere of an agricultural soil. Front Microbiol 7:1524

Kramer S, Marhan S, Haslwimmer H, Ruess L, Kandeler E (2013) Temporal variation in surface and subsoil abundance and function of the soil microbial community in an arable soil. Soil Biol Biochem 61:76–85

Lee KCY, Dunfield PF, Stott MB (2014) The phylum Armatimonadetes. In: Rosenberg E, DeLong EF, Lory S, Stackebrandt E, Thompson F (eds) The prokaryotes: other major lineages of bacteria and the archaea. Springer, Berlin, pp 447–458

Lehmann J, Hansel CM, Kaiser C, Kleber M, Maher K, Manzoni S, Nunan N, Reichstein M, Schimel JP, Torn MS, Wieder WR, Kögel-Knabner I (2020) Persistence of soil organic carbon caused by functional complexity. Nat. Geosci 13:529–534

Leinemann T, Preusser S, Mikutta R, Kalbitz K, Cerlie C, Höschen C, Mueller CW, Kandeler E, Guggenberger G (2018) Multiple exchange processes on mineral surfaces control the transport of dissolved organic matter through soil profiles. Soil Biol Biochem 218: 79–90

Liliensiek AK, Thakuria D, Clipson N (2012) Influences of plant species composition, fertilisation and *Lolium perenne* ingression on soil microbial community structure in three Irish grasslands. Microb Ecol 63:509–521

Ma W, Peng D, Walker SL, Cao B, Gao C-H, Huang Q, Cai P (2017) Bacillus subtilis biofilm development in the presence of soil clay minerals and iron oxides. npj Biofilms Microbiomes 3:1–9

Marhan S, Kandeler E, Rein S, Fangmeier A, Niklaus PA (2010) Indirect effects of soil moisture reverse soil C sequestration responses of a spring wheat agroecosystem to elevated CO_2. Glob Chang Biol 16: 469–483

McNamara NP, Black HIJ, Beresford NA, Parekh NR (2003) Effects of acute gamma irradiation on chemical, physical and biological properties of soils. Appl Soil Ecol 24:117–132

Mueller T, Joergensen RG, Meyer B (1992) Estimation of soil microbial biomass C in the presence of living roots by fumigation-extraction. Soil Biol Biochem 24:179–181

Müller K, Kramer S, Haslwimmer H, Marhan S, Scheunemann N, Butenschoen O, Scheu S, Kandeler E (2016) Carbon transfer from maize roots and litter into bacteria and fungi depends on soil depth and time. Soil Biol Biochem 93:79–89

Müller K, Marhan S, Kandeler E, Poll C (2017) Carbon flow from litter through soil microorganisms: from incorporation rates to mean residence times in bacteria and fungi. Soil Biol Biochem 115:187–196

Parikh SJ, Goyne KW, Margenot AJ, Mukome FND, Calderó, FJ (2014) Chapter one - soil chemical insights provided through vibrational spectroscopy. In Advances in agronomy. Sparks, DL (ed): Academic Press, pp 1–148

Paterson E, Osler G, Dawson LA, Gebbing T, Sim A, Ord B (2008) Labile and recalcitrant plant fractions are utilised by distinct microbial communities in soil: independent of the presence of roots and mycorrhizal fungi. Soil Biol Biochem 40:1103–1113

Pausch J, Hünninghaus M, Kramer S, Scharroba A, Scheunemann N, Butenschoen O, Marhan S, Bonkowski M, Kandeler E, Scheu S, Kuzyakov Y, Ruess L (2018) Soil depth rather than litter addition determines carbon budgets of food webs in an arable soil. Pedobiologia 69:29–33

Pausch J, Kramer S, Scharroba A, Scheunemann N, Butenschoen O, Kandeler E, Marhan S, Riederer M, Scheu S, Kuzyakov Y, Ruess L (2015) Small but active – the fungal channel drives carbon flow in the food web of an arable soil. Func Ecol 30:479–489

Poll C, Marhan S, Ingwersen J, Kandeler E (2008) Dynamics of carbon turnover and microbial abundance in a rye detritusphere. Soil Biol Biochem 40:1306–1321

Purcell EM (1977) Life at low Reynolds number. Am J Phys 45:3–11

R Core Team (2019) R: A language and environment for statistical computing. In: Vienna, Austria: R foundation for statistical computing

Rosenberg E, DeLong EF, Lory S, Stackebrandt E, Thompson F (2013) The prokaryotes. Springer, Berlin

Rousk J, Bååth E (2007) Fungal and bacterial growth in soil with plant materials of different C/N ratios. FEMS Microbiol Ecol 62:258–267

Rousk J, Brookes PC, Bååth E (2009) Contrasting soil pH effects on fungal and bacterial growth suggest functional redundancy in carbon mineralization. Appl Env Microbiol 75:1589–1596

Rovira AD (1969) Plant root exudates. Bot Rev 35:35–57

Ruess L, Chamberlain PM (2010) The fat that matters: soil food web analysis using fatty acids and their carbon stable isotope signature. Soil Biol Biochem 42:1898–1910

Seaton FM, George PBL, Lebron I, Jones DL, Creer S, Robonson DA (2020) Soil textural heterogeneity impacts bacterial but not fungal diversity. Soil Biol Biochem 144:107766

Simon A, Bindschedler S, Job D, Wick LY, Filippidou S, Kooli WM, Verrecchia EP, Junier P (2015) Exploiting the fungal highway: development of a novel tool for the in situ isolation of bacteria migrating along fungal mycelium. FEMS Microbiol Ecol 91:fiv116

Simon A, Hervé V, Al-Dourobi A, Verrecchia E, Junier P (2017) An in situ inventory of fungi and their associated migrating bacteria in forest soils using fungal highway columns. FEMS Microbiol Ecol 93:fiw217

Simonin A, Palma-Guerrero J, Fricker M, Glass NL (2012) Physiological significance of network organization in fungi. Eukaryotic Cell 11: 1345–1352

Smith NW, Shorten PR, Altermann E, Roy NC, McNabb WC (2019) The classification and evolution of bacterial cross-feeding. Front Ecol Evol 7:153

Stotzky G (1986) Influence of soil mineral colloids on metabolic processes, growth, adhesion, and ecology of microbes and viruses. In: Huang PM, Schnitzer M (eds) Interactions of soil minerals with natural organics and microbes. Soil Science Society of America, Madison, pp 305–428

Strickland MS, McCulley RL, Nelson JA, Bradford MA (2015) Compositional differences in simulated root exudates elicit a limited functional and compositional response in soil microbial communities. Front Microbiol 6:817

Sun Q, Liu X, Wang S, Lian B (2020) Effects of mineral substrate on ectomycorrhizal fungal colonization and bacterial community structure. Sci Total Environ 721:137663

Tecon R, Or D (2017) Biophysical processes supporting the diversity of microbial life in soil. FEMS Microbiol Rev 41:599–623

Thompson LR, Sanders JG, McDonald D, Amir A, Ladau J, Locey KJ, Prill RJ, Tripathi A, Gibbons SM, Ackermann G, Navas-Molina JA, Janssen S, Kopylova E, Vázquez-Baeza Y, González A, Morton JT, Mirarab S, Zech Xu Z, Jiang L, Haroon MF, Kanbar J, Zhu Q, Jin Song S, Kosciolek T, Bokulich NA, Lefler J, Brislawn CJ, Humphrey G, Owens SM, Hampton-Marcell J, Berg-Lyons D, McKenzie V, Fierer N, Fuhrman JA, Clauset A, Stevens RL, Shade A, Pollard KS, Goodwin KD, Jansson JK, Gilbert JA, Knight R, The Earth Microbiome Project consortium (2017) A communal catalogue reveals Earth's multiscale microbial diversity. Nature 551:457–463

Totsche KU, Rennert T, Gerzabek MH, Kögel-Knabner I, Smalla K, Spiteller M, Vogel HJ (2010) Biogeochemical interfaces in soil: the interdisciplinary challenge for soil science. J Plant Nutr Soil Sc 173:88–99

Uksa M, Schloter M, Endesfelder D, Kublik S, Engel M, Kautz T, Köpke U, Fischer D (2015) Prokaryotes in subsoil-evidence for a strong spatial separation of different phyla by analysing co-occurrence networks. Front Microbiol 6:1269

Uroz S, Kelly LC, Turpault MP, Lepleux C, Frey-Klett P (2015) The mineralosphere concept: mineralogical control of the distribution and function of mineral-associated bacterial communities. Trends Microbiol 23:751–762

Van Hees PA, Jones DL, Finlay R, Godbold DL, Lundström US (2005) The carbon we do not see - the impact of low molecular weight compounds on carbon dynamics and respiration in forest soils: a review. Soil Biol Biochem 37:1–13

Vance ED, Brookes PC, Jenkinson DS (1987) An extraction method for measuring soil microbial biomass C. Soil Biol Biochem 19:703–707

Venables WN, Ripley BD (2002) Modern applied statistics with S. Fourth Edition. Springer, New York

Vieira S, Sikorski J, Dietz S, Herz K, Schrumpf M, Bruelheide H, Scheel D, Friedrich MW, Overmann J (2020) Drivers of the composition of active rhizosphere bacterial communities in temperate grasslands. ISME J 14:463–475

Vieira S, Sikorski J, Gebala A, Boeddinghaus RS, Marhan S, Rennert T, Kandeler E, Overmann J (2020) Bacterial colonization of minerals in grassland soils is selective and highly dynamic. Environ Microbiol 22:917–933

Vogel C, Babin D, Pronk GJ, Heister K, Smalla K, Kögel-Knabner I (2014) Establishment of macro-aggregates and organic matter turnover by microbial communities in long-term incubated artificial soils. Soil Biol Biochem 79:1–11

Wang T, Tian Z, Bengtson TA, Persson P (2017) Mineral surface-reactive metabolites secreted during fungal decomposition contribute to the formation of soil organic matter. Environ Microbiol 19:5117–5129

Wang X, Toner BM, Yoo K (2019) Mineral vs. organic matter supply as a limiting factor for the formation of mineral-associated organic matter in forest and agricultural soils. Sci Total Environ 692:344–353

Whiteside MD, Werner GDA, Caldas VEA, van't Padje A, Dupin SE, Elbers B, Bakker M, Wyatt GAK, Klein M, Hink MA, Postma M, Vaitla B, Noë R, Shimizu TS, West SA, Kiers ET (2019) Mycorrhizal fungi respond to resource inequality by moving phosphorus from rich to poor patches across networks. Curr Biol 29:2043–2050

Whitman T, Neurath R, Perera A, Chu-Jacoby I, Ning D, Zhou J, Nico P, Pett-Ridge J, Firestone M (2018) Microbial community assembly differs across minerals in a rhizosphere microcosm. Environ Microbiol 20:4444–4460

Yang P, Van Elsas JD (2018) Mechanisms and ecological implications of the movement of bacteria in soil. Appl Soil Ecol 129:112–120

Zelles L (1997) Phospholipid fatty acid profiles in selected members of soil microbial communities. Chemosphere 35:275–294

Zelles L (1999) Fatty acid patterns of phospholipids and lipopolysaccharides in the characterisation of microbial communities in soil: a review. Biol Fertil Soil 29:111–129